Available online at www.sciencedirect.com

ScienceDirect

Current Opinion in Neurobiology

New insights on the structure of alpha-synuclein fibrils using cryo-electron microscopy

Ricardo Guerrero-Ferreira[1,2], Lubomir Kovacik[2], Dongchun Ni[2] and Henning Stahlberg[2]

Fibrils of alpha-synuclein are significant components of cellular inclusions associated with several neuropathological disorders including Parkinson's disease, multiple system atrophy and dementia with Lewy bodies. In recent years, technological advances in the field of transmission electron microscopy and image processing have made it possible to solve the structure of alpha-synuclein fibrils at high resolution. This review discusses the results of structural studies using cryo-electron microscopy, which revealed that in-vitro produced fibrils vary in diameter from 5 nm for single-protofilament fibrils, to 10 nm for two-protofilament fibrils. In addition, the atomic models hint at contributions of the familial Parkinson's disease mutation sites to inter-protofilament interaction and the locations where post-translational modifications take place. Here, we propose a nomenclature system that allows identifying the existing alpha-synuclein polymorphs and that will allow to incorporate additional high-resolution structures determined in the future.

Addresses
[1] Robert P. Apkarian Integrated Electron Microscopy Core, Emory University School of Medicine, 1521 Dickey Drive NE, Atlanta, Georgia 30322, USA

[2] Center for Cellular Imaging and NanoAnalytics (C-CINA), Biozentrum, University of Basel, Mattenstrasse 26, 4058 Basel, Switzerland

Corresponding author:
Stahlberg, Henning (henning.stahlberg@unibas.ch)

Current Opinion in Neurobiology 2020, **61**:89–95

This review comes from a themed issue on **Neurobiology of disease**

Edited by **Michel Goedert** and **Christian Haass**

For a complete overview see the Issue and the Editorial

Available online 26th February 2020

https://doi.org/10.1016/j.conb.2020.01.014

Introduction

Studies of the structure of amyloid fibrils have been pivotal in understanding the mechanism of their formation and growth, and in establishing approaches for the development of vaccine and therapeutic alternatives to fight diseases caused by amyloids. The protein alpha-synuclein (aSyn) has been identified as one of the components of Lewy bodies (LB) and Lewy neurites (LN), which are cellular inclusions characteristic of synucleinopathies including Parkinson's disease (PD) [1–4]. Recently, Shahmoradian *et al.* studied Lewy bodies from post-mortem human brain by correlative light and electron microscopy (CLEM), and reported that the main structural component of Lewy bodies are membrane fragments, whereas filamentous structures were only seen, to a limited extent, in a smaller subset of Lewy bodies. The membranous Lewy bodies were not noticeable by electron microscopy alone due to their texture being highly similar to that of the surrounding tissue, so that guidance by CLEM was required to localize these. Nevertheless, prionoid fibrils of the protein aSyn are existing in human brain of PD patients [1,2,5], and in addition are expected to exist in several other neurodegenerative diseases related to aSyn [6–8].

Alpha-synuclein is part of the synuclein family of proteins, related by sequence homology, which include also beta-synuclein and gamma-synuclein [3,5,9]. The sequence homology between these is higher at their amino-terminal regions, which also contain 5–6 lipid-binding repeats [10].

The process of aSyn fibrillar structure initiation is not fully understood. Some evidence suggests that fibril formation begins with destabilization of aggregation-resistant, helical tetrameric forms, followed by monomeric aSyn misfolding and aggregation into fibrils [11,12]. However, other studies have also shown monomeric and not tetrameric aSyn in human and rodent central nervous system, and monomeric aSyn was found in mouse and rat brains and mammalian cell lines with human aSyn expressed [13]. It is possible that structural changes occur in aSyn within the cellular milieu due to protein activity or the interaction of aSyn with biological membranes, and that both, monomers, tetramers and possibly even certain strain types of fibrils occur within the cell in dynamic equilibrium. It is currently unknown, if the *in vitro* generated fibril strains described here are also present in human brain, or if brain-derived fibrils occupy a different fold all together. The latter was found for tau, where brain-derived fibrils showed a radically different conformation to what had been previously suggested based on *in vitro* generated tau fibrils [14–16]. A combination of cryo-electron microscopy (cryo-EM) and cryo-electron tomography could prove useful in determining the composition of aSyn forms within cells or tissue, provided that a conservative sample preparation protocol is applied [17].

Besides cryo-EM, insights into aSyn structure have been obtained through nuclear magnetic resonance (NMR) [18–28], micro-electron diffraction (micro-ED) [29], and through quenched hydrogen/deuterium (H/D) exchange [23]. In this review, we describe how the application of these techniques has resulted in a better understanding of the structure of aSyn fibrils, and discuss hypotheses on a mechanism of fibril aggregation and growth, the role of the known familial Parkinson's disease mutations in aSyn, and potential strategies to disrupt formed fibrils or arrest the fibrillization process (Table 1).

The structure of alpha-synuclein

The protein alpha-synuclein is composed of 140 amino acids (Figure 1). Residues 1–60 encompass the lysine-rich N-terminus, which contains the KTK lipid-binding repeats responsible for vesicle binding [30–32]. In addition, familial mutations of the SNCA gene are found in this region, including A30P [33], E46K [34], H50Q [35], G51D [36], A53E [37], A53V [38] and A53T [39].

The central group of aSyn aminoacids ranging from residues 61–95 are known as the non-amyloid-ß component (NAC) region [40,41]. This region is responsible for fibril aggregation, as initially demonstrated by Li *et al.* [42], who showed that proteins with the NAC region have the ability to switch from a random coil state to a highly hydrophobic, easily aggregating beta-sheet state. This evidence was confirmed by the finding that beta-synuclein, which compared to alpha-synuclein lacks 12 aminoacids (residues 71–82) in the NAC region, is not capable of fibrilization [3,5].

Residues 96–140 of aSyn encompass the highly negatively charged C-terminal region, which is necessary for calcium binding [23,43,44]. Interestingly, while truncation of this domain has been shown to promote fibril formation, which may indicate its role in aSyn pathology [45–48], inhibition of truncation of this domain has reduced neurodegeneration in a transgenic mouse model of MSA [7].

Various biophysical and biochemical approaches including solid-state and solution-state NMR, Electron Paramagnetic Resonance (EPR), and limited proteolysis have been employed to understand the composition of aSyn fibrils [10,23,49,50]. These studies revealed that aSyn fibrils are made of more than one protofilament, vary in diameter from 5 to 10 nm, and can occupy more than one polymorph. The first 30 residues of individual aSyn monomers are heterogeneous, residues 31–109 are folded, and the C-terminal residues 110–140 are flexible.

Alpha-synuclein polymorphism and familial Parkinson's disease mutations

Cryo-EM investigations have allowed localizing familial PD mutations of aSyn in the context of the fibril. In all atomic structures known to date, mutation sites are involved in either the interaction between protofilaments or the stability of monomeric conformations, which may hint at the role that these changes play on fibril formation and growth.

Overall, in polymorph 1a structures [51••,52••,53••], three mutation sites within the atomic model participate in the tight interface between protofilaments (Figure 1). Of them, the E46 residue markedly contributes to aSyn folding stability by strongly interacting with the lysine in position 80, forming a salt bridge in polymorph 1a. The E46K change of a glutamic acid to a lysine would likely result in electrostatic repulsion and destabilization of the monomer conformation. In contrast, polymorph 1b protofilaments [53••] interact via residues V66-A78, relocating the mutation sites to the periphery of the fibril. However, the E46 residue interacts with another glutamic acid in position 83, indicating that the E46K mutation would lead to the formation of a stabilizing salt bridge. In polymorphs 2a and 2b, E46 is one of the main residues contributing to the interface between the two

Table 1

Comparison of cryo-EM alpha-synuclein fibril structures

Reference	[51••]	[52••]	[53••]	[53••]	[54•]	[54•]	[55••]	[55••]
Modification	C-terminally truncated	N-terminally acetylated	wild-type	wild-type	H50Q	H50Q	wild-type	wild-type
Polymorph	1a	1a	Rod (1a)	Twister (1b)	Narrow (1c)	Wide (1d)	2a	2b
Number of residues in atomic model	57	62	60	41	63	63	71	71
Protofibril interface residues	H50-E57	H50-E57	H50-E57	V66-A78	Single protofilament	T59-K60	K45-E57	K45-E46
Mutation sites localized	E46K H50K G51D A53T	E46K H50K G51D A53T	E46K H50K G51D A53T	E46K H50K G51D A53T	E46K H50K G51D A53T	E46K H50K G51D A53T	E46K H50K G51D A53T	E46K H50K G51D A53T
Helical rise (Å)	2.45	2.40	2.40	2.40	4.81	4.82	4.80	2.40
Helical twist (°)	179.5	179.63	179.53	179.06	−0.97	−0.83	−0.80	179.55
Resolution (Å)	3.42	3.07	3.70	3.70	3.30	3.6	2.99	3.39
EMDB	EMD-0148	EMD-6988	EMD-7618	EMD-7619	EMD-20328	EMD-20331	EMD-10307	EMD-10305
PDB	6H6B	6A6B	6CU7	6CU8	6PEO	6PES	6SSX	6SST

Figure 1

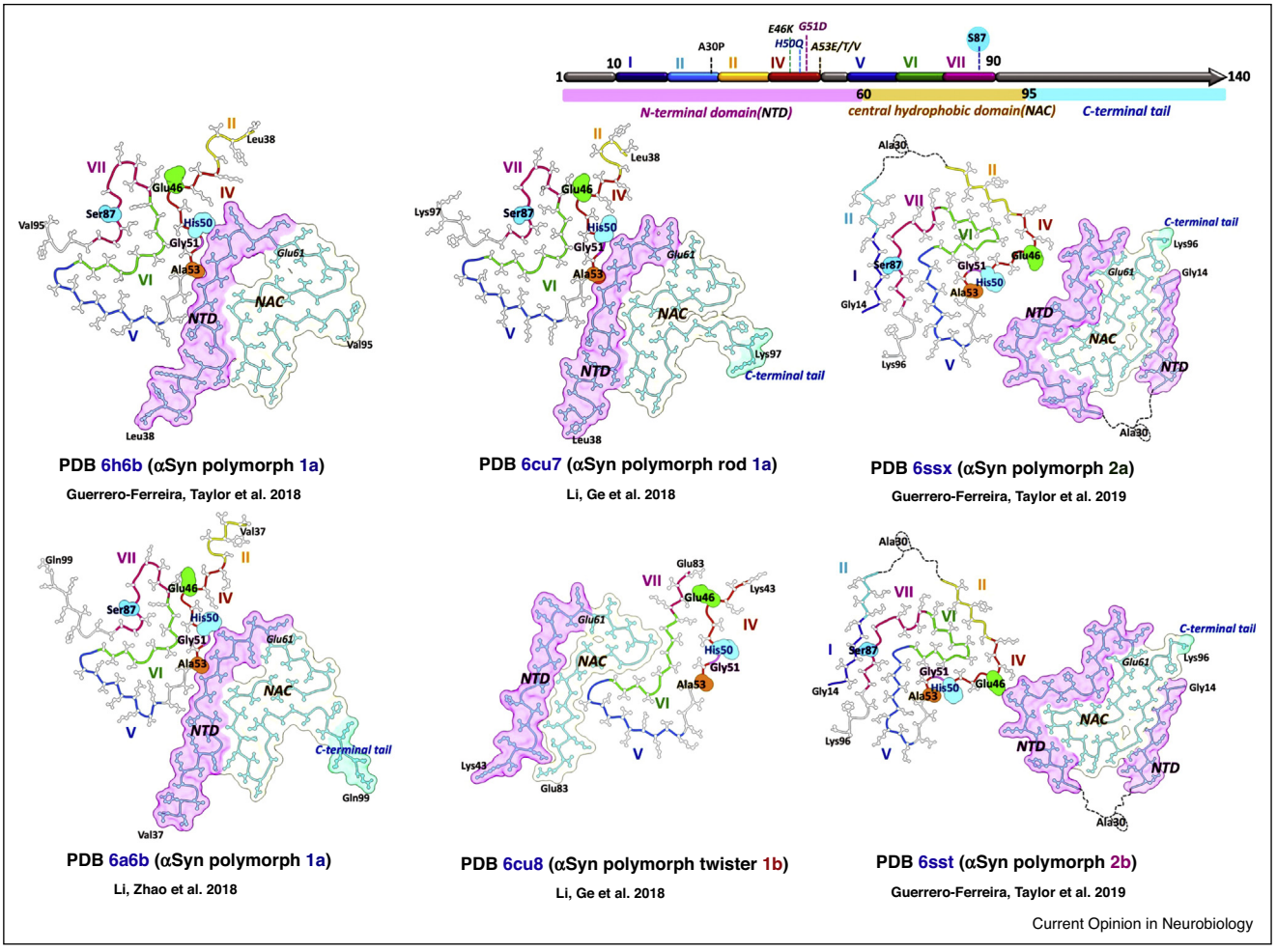

Comparison of cryo-EM structures of six wild-type aSyn polymorphs. The nomenclature proposed in this review is used in addition to the names proposed in the respective original publications. PDB accession numbers are indicated. Atomic models in protofilaments are represented as ribbons and sticks with one protofilament including a transparent surface with the N-terminal domain in pink, the NAC region in white and the C-terminal tail in blue. Familial PD mutation sites are indicated on the top diagram, as well as on each polymorph with matching colors. In addition, seven repeat sequences are shown as a color sequence in the top diagram as well as in the atomic models. First and last residues of each model are also indicated.

protofilaments. Particularly in polymorph 2b, where only a narrow connection between K45 and E46 on one protofibril, to E46 and K45 on the other protofibril maintain the interface, the E46K mutation with an additional lysine in the site of inter-protofilament interaction would make this polymorph unlikely.

In polymorphs 1c (narrow fibrils) and 1d (wide fibrils) [54••] the structure of the common kernel for class 1 polymorphs is maintained. In addition, polymorph 1c closely resembles the solid-state NMR structure published by Tuttle *et al.* [24] in that it forms a 5 nm thick fibril and a salt bridge between E46 and K80. These two polymorphs were obtained from aSyn fibrils carrying the H50Q mutation, which causes familial late-onset PD. This mutation is likely to produce an effect similar to the E46K mutation on fibril stability. Polymorph 1a is made out of two protofilaments that interact through residues H50 to E57 and requires the H50 residue to form a salt bridge with E57 to maintain inter-protofilament interaction. The H50Q mutation would destabilize this bond due to the presence of a polar, uncharged glutamine instead of a positively charged histidine. In contrast, the interaction between residues H50 and K45, which contributes to the aSyn fold, is not affected by the H50Q mutation, as shown by Boyer *et al.* [54••], who also confirmed the transition of the polymorph 1a protofilament interface to either a narrow fibril (polymorph 1c) formed by a single protofilament or a wide fibril (polymorph 1d) in which the interface is comprised only of residues T59 and K60.

The G51D mutation triggers early onset Parkinson's disease. The steric hindrance resulting from the replacement of the glycine in position 50 by a large, negatively charged aspartic acid in this mutant is likely to disturb the steric zipper maintaining the stability of the fibril in polymorph 1a. In contrast, residue G51 in polymorphs 1b, 2a and 2b is positioned in such a way that it is not likely to affect the strength of inter-protofilament interaction. However, the aspartic acid G51 is in all fibril polymorphs oriented towards the inner core of the protofibrils, where it establishes a contact with the NAC region. The G51D mutation should therefore disrupt the inter-beta-strand contact in the beta-sheets, so that fibrils with a different protofibril conformation are expected.

The A53T and A53E early-onset familial PD mutations replace the small alanine side chain in A53 with a larger, polar threonine (A53T), or to a negatively charged glutamic acid (A53E), respectively. This would result in a reduction of hydrophobic interaction similar to that of the G51D mutation. Mutation to a larger, non-polar valine (A53V) would increase hydrophobicity in the steric zipper region but the bulkier side-chain size would create a steric hindrance in the region which may affect the interaction between protofilaments. In this context, the structure of the aSyn polymorph 1a would be affected by these mutations. However, the core of polymorph 1b, in which protofilaments interact through residues in the NAC region, would be unaffected by the aforementioned A53 mutations. Similarly, the location of A53 in polymorphs 2a and 2b makes mutations on these sites unlikely to affect inter-protofilament interaction but may disfavor fibril aggregation by affecting the distribution of hydrophobic pockets in individual aSyn molecules.

Alpha-synuclein polymorphism and disease-related post-translational modifications

Solving the structure of aSyn fibrils by cryo-EM allowed identification of post-translational, disease-associated modifications. In Parkinson's disease, these modifications have been correlated with Lewy body formation, not only in postmortem human tissue, but also in transgenic mouse models of Parkinson's disease and other synucleinopathies. These modifications, which include phosphorylation, ubiquitination, cross-linking or C-terminal truncation, may inhibit fibrillization, suggesting that they are late events occurring after protein aggregation [56].

Ubiquitination affects mostly lysines 21, 23, 32 and 34, which reside within the N-terminal region of aSyn [57,58]. Because of the disordered nature of this region, these residues fall outside of the atomic structures solved by cryo-EM, with the exception of polymorphs 2a and 2b, where K21 and K23 mark the end of a beta-sheet that interacts (i) with the NAC region and (ii) with the beginning of a disordered stretch of residues ending with a glutamic acid in position 35. However, the side chains of K21 and K23 in polymorphs 2a and 2b are oriented towards the inside of the fibril core and should therefore be inaccessible to ubiquitin in these polymorphs.

Acetylation is another post-translational modification restricted to the N-terminus of aSyn. It occurs in mammalian cells and has been shown to improve lipid binding affinity, N-terminal helicity, as well as reduce the rate of aggregation [59,60]. The structures of polymorphs 1a, 2a and 2b have been obtained by cryo-EM from N-terminally acetylated, recombinant aSyn, indicating that this modification does not affect the fold of these fibrils.

All available atomic resolution aSyn structures except for polymorph 1b include the phosphorylation site serine 87, which is the only phosphorylation site of alpha synuclein located within the NAC region [61,62]. In polymorph 1a [51••,52••,53••,55••], S87 faces the periphery of the fibril which makes it amenable for post-translational modification. In contrast, in both 1c and 1d polymorphs [54••] and the solid-state NMR structure [24], S87 appears with its side chain facing the inside of the protofilament core. Interestingly, in the structures of polymorphs 2a and 2b, a beta-sheet was solved which corresponds to a stretch of N-terminal residues and associates with the NAC core, thus making S87 inaccessible to any modification. In addition, the connection between residues A17, A18 and A19 and S87 was confirmed by solid-state NMR data [55••].

Data processing of cryo-EM data

Cryo-EM images for structural analysis of amyloid fibrils are typically collected in the same way as for other proteins. Using state-of-the-art cryo-transmission electron microscopes driven by automated routines, several thousands of images of protein samples frozen in thin layers of vitrified buffer solution are recorded with direct-detection cameras as stacks of 40–60 dose-fractionated image frames. Data are typically recorded at a pixel size of ~1 Å or smaller, which limits the resolution of the image to 1/[2 Å] or higher, thus safely allowing for discrimination of the typical 4.8 Å helical rise and for the atomic structure of the fibrils.

The helical symmetry of filamentous samples made the first three-dimensional structure reconstruction from two-dimensional electron micrographs possible [63]. Since then, helical image processing has been further developed, resulting into several modern software packages, including the Burnham-Brandeis Helical Package [64], IHRSR [65], Phoelix [66], Spring [67], and Relion [68]. Among these, the Relion program employing the Bayesian probability approach has become a standard tool for structural determination of cryo-EM protein structures. Since the introduction of its helical reconstruction extension by He *et al.* [69•], Relion has also become the most frequently used program for solving the structure of

helical assemblies. It offers all tools needed for helical reconstruction, as it provides interface to routines performing motion correction of image stacks, determination of contrast-transfer function (CTF) parameters, selection of filaments, and the 2D and 3D processing of extracted helical segments. In addition, the Relion-specific resolution-boosting routines for per-particle CTF determination and motion correction can also be employed for helices.

In Relion, segments of straight filaments are manually picked from images displaying recognizable 4.8 Å line reflections in their computed power spectra. Alternatively, automated particle picking programs such as Gautomatch (www.mrc-lmb.cam.ac.uk/kzhang/Gautomatch/), Topaz [70], or SPHIRE-crYOLO [71] can be also used to detect helical segments in a manner comparable to the single-particle protocol. The SPRING package also offers the MICHELIXTRACE program for automated filament detection.

Individual helical particles are extracted from marked filaments as square boxes with box spacing corresponding to an integer multiple of the helical rise parameter of the aSyn fiber. Its helical rise is determined by the length of hydrogen bonds between two consecutive aSyn β-strands (~4.8 Å). The extracted fibers are subjected to 2D classification, which allows recognizing the difference between single or double protofilament fibrils, and in the latter case can reveal if the two opposing aSyn protofilaments are arranged head-to-head with a typical helical rise of 4.8 Å and a twist between −1 and 0°, or in a steric zipper with a helical rise of ~2.4 Å and a twist between 179 and 179.7 °. In 3D processing in Relion, the initial rough values of helical rise and twist are refined to final values. As starting models, former aSyn structures, low-pass-filtered to 40 or 50 Å can be used, as well as synthetic cylindrical models that can be generated with the relion_helix_toolbox program that is part of the Relion set of processing tools. Despite significant recent advances in the computational tools, the 3D refinement of the structure of amyolid fibrils is still challenging, due to the relatively flat energy landscape with several local optima for the refinements. Scheres [72] has recently provided a collection of helical processing approaches and tools in RELION-3.1 for the correct estimation of helical parameters of fibrils under study, which is a great resource for the processing of helical filament datasets.

Conclusion

Cryo-electron microscopy has matured into an efficient tool to determine the structure of proteins, macromolecular complexes and filamentous structures at high resolution. In the case of amyloid fibrils associated with neuropathological disorders, cryo-EM has become the method of choice for elucidating the atomic structures of fibrils prepared from recombinant proteins or fibrils directly isolated from post-mortem brain tissue. Isolation of aSyn fibrils from brain at concentrations required for cryo-EM analysis has so far not been achieved. However, recombinantly produced aSyn protein can be provoked to aggregate into fibrils *in vitro* under specific conditions, and their structures can be analyzed using cryo-EM. Structural knowledge about the fibril space of aSyn protein will prove useful, once a brain-derived cryo-EM fibril structure is available.

We here propose a categorization of aSyn fibril polymorphs based on the organization of the beta sheets (polymorph numbers 1, 2, etc.), and on the nature of protofilament interaction (a, b, etc.). This system allows extension with possible further structures, as previously suggested [55••] and already ratified in the review by Meade *et al.* [4]. This identification system will be useful for tracking of structures in the various databases.

Conflict of interest statement

Nothing declared.

Acknowledgement

This work was supported by the Swiss National Science Foundation (grants 310030_188548/1 and CRSII5_177195/1).

References

1. Spillantini MG, Schmidt ML, Lee VM, Trojanowski JQ, Jakes R, Goedert M: **Alpha-synuclein in Lewy bodies**. *Nature* 1997, **388**:839-840.
2. Spillantini MG, Crowther RA, Jakes R, Hasegawa M, Goedert M: **α-Synuclein in filamentous inclusions of Lewy bodies from Parkinson's disease and dementia with Lewy bodies**. *Proc Natl Acad Sci U S A* 1998, **95**:6469-6473.
3. Stefanis L: **Alpha-synuclein in Parkinson's disease**. *Cold Spring Harb Perspect Med* 2012, **2**:a009399.
4. Meade RM, Fairlie DP, Mason JM: **Alpha-synuclein structure and Parkinson's disease - lessons and emerging principles**. *Mol Neurodegener* 2019, **14**:29.
5. Jakes R, Spillantini MG, Goedert M: **Identification of two distinct synucleins from human brain**. *FEBS Lett* 1994, **345**:27-32.
6. Arima K, Ueda K, Sunohara N, Arakawa K, Hirai S, Nakamura M, Tonozuka-Uehara H, Kawai M: **NACP/alpha-synuclein immunoreactivity in fibrillary components of neuronal and oligodendroglial cytoplasmic inclusions in the pontine nuclei in multiple system atrophy**. *Acta Neuropathol* 1998, **96**:439-444.
7. Bassil F, Fernagut P-O, Bezard E, Pruvost A, Leste-Lasserre T, Hoang QQ, Ringe D, Petsko GA, Meissner WG: **Reducing C-terminal truncation mitigates synucleinopathy and neurodegeneration in a transgenic model of multiple system atrophy**. *Proc Natl Acad Sci U S A* 2016, **113**:9593-9598.
8. Campbell BC, McLean CA, Culvenor JG, Gai WP, Blumbergs PC, Jakala P, Beyreuther K, Masters CL, Li QX: **The solubility of alpha-synuclein in multiple system atrophy differs from that of dementia with Lewy bodies and Parkinson's disease**. *J Neurochem* 2001, **76**:87-96.
9. Clayton DF, George JM: **The synucleins: a family of proteins involved in synaptic function, plasticity, neurodegeneration and disease**. *Trends Neurosci* 1998, **21**:249-254.

10. Der-Sarkissian A, Jao CC, Chen J, Langen R: **Structural organization of alpha-synuclein fibrils studied by site-directed spin labeling**. *J Biol Chem* 2003, **278**:37530-37535.

11. Bartels T, Choi JG, Selkoe DJ: **Alpha-synuclein occurs physiologically as a helically folded tetramer that resists aggregation**. *Nature* 2011, **477**:107-110.

12. Nuber S, Rajsombath M, Minakaki G, Winkler J, Muller CP, Ericsson M, Caldarone B, Dettmer U, Selkoe DJ: **Abrogating native alpha-synuclein tetramers in mice causes a L-DOPA-responsive motor syndrome closely resembling Parkinson's disease**. *Neuron* 2018, **100**:75-90 e75.

13. Fauvet B, Mbefo MK, Fares MB, Desobry C, Michael S, Ardah MT, Tsika E, Coune P, Prudent M, Lion N *et al.*: **Alpha-synuclein in central nervous system and from erythrocytes, mammalian cells, and *Escherichia coli* exists predominantly as disordered monomer**. *J Biol Chem* 2012, **287**:15345-15364.

14. Falcon B, Zhang W, Murzin AG, Murshudov G, Garringer HJ, Vidal R, Crowther RA, Ghetti B, Scheres SHW, Goedert M: **Structures of filaments from Pick's disease reveal a novel tau protein fold**. *Nature* 2018, **561**:137-140.

15. Falcon B, Zivanov J, Zhang W, Murzin AG, Garringer HJ, Vidal R, Crowther RA, Newell KL, Ghetti B, Goedert M *et al.*: **Novel tau filament fold in chronic traumatic encephalopathy encloses hydrophobic molecules**. *Nature* 2019, **568**:420-423.

16. Fitzpatrick AWP, Falcon B, He S, Murzin AG, Murshudov G, Garringer HJ, Crowther RA, Ghetti B, Goedert M, Scheres SHW: **Cryo-EM structures of tau filaments from Alzheimer's disease**. *Nature* 2017, **547**:185-190.

17. Lewis AJ, Genoud C, Pont M, van de Berg WD, Frank S, Stahlberg H, Shahmoradian SH, Al-Amoudi A: **Imaging of post-mortem human brain tissue using electron and X-ray microscopy**. *Curr Opin Struct Biol* 2019, **58**:138-148.

18. Gath J, Bousset L, Habenstein B, Melki R, Böckmann A, Meier BH: **Unlike twins: an NMR comparison of two alpha-synuclein polymorphs featuring different toxicity**. *PLoS One* 2014, **9**: e90659.

19. Gath J, Bousset L, Habenstein B, Melki R, Meier BH, Böckmann A: **Yet another polymorph of alpha-synuclein: solid-state sequential assignments**. *Biomol NMR Assign* 2014, **8**:395-404.

20. Gath J, Habenstein B, Bousset L, Melki R, Meier BH, Böckmann A: **Solid-state NMR sequential assignments of alpha-synuclein**. *Biomol NMR Assign* 2012, **6**:51-55.

21. Verasdonck J, Bousset L, Gath J, Melki R, Böckmann A, Meier BH: **Further exploration of the conformational space of alpha-synuclein fibrils: solid-state NMR assignment of a high-pH polymorph**. *Biomol NMR Assign* 2016, **10**:5-12.

22. Bousset L, Pieri L, Ruiz-Arlandis G, Gath J, Jensen PH, Habenstein B, Madiona K, Olieric V, Böckmann A, Meier BH *et al.*: **Structural and functional characterization of two alpha-synuclein strains**. *Nat Commun* 2013, **4**:2575.

23. Vilar M, Chou HT, Luhrs T, Maji SK, Riek-Loher D, Verel R, Manning G, Stahlberg H, Riek R: **The fold of alpha-synuclein fibrils**. *Proc Natl Acad Sci U S A* 2008, **105**:8637-8642.

24. Tuttle MD, Comellas G, Nieuwkoop AJ, Covell DJ, Berthold DA, Kloepper KD, Courtney JM, Kim JK, Barclay AM, Kendall A *et al.*: **Solid-state NMR structure of a pathogenic fibril of full-length human alpha-synuclein**. *Nat Struct Mol Biol* 2016, **23**:409-415.

25. Comellas G, Lemkau LR, Zhou DH, George JM, Rienstra CM: **Structural intermediates during alpha-synuclein fibrillogenesis on phospholipid vesicles**. *J Am Chem Soc* 2012, **134**:5090-5099.

26. Comellas G, Lemkau LR, Nieuwkoop AJ, Kloepper KD, Ladror DT, Ebisu R, Woods WS, Lipton AS, George JM, Rienstra CM: **Structured regions of alpha-synuclein fibrils include the early-onset Parkinson's disease mutation sites**. *J Mol Biol* 2011, **411**:881-895.

27. Lv G, Kumar A, Giller K, Orcellet ML, Riedel D, Fernandez CO, Becker S, Lange A: **Structural comparison of mouse and human alpha-synuclein amyloid fibrils by solid-state NMR**. *J Mol Biol* 2012, **420**:99-111.

28. Heise H, Hoyer W, Becker S, Andronesi OC, Riedel D, Baldus M: **Molecular-level secondary structure, polymorphism, and dynamics of full-length alpha-synuclein fibrils studied by solid-state NMR**. *Proc Natl Acad Sci U S A* 2005, **102**:15871-15876.

29. Rodriguez JA, Ivanova MI, Sawaya MR, Cascio D, Reyes FE, Shi D, Sangwan S, Guenther EL, Johnson LM, Zhang M *et al.*: **Structure of the toxic core of alpha-synuclein from invisible crystals**. *Nature* 2015, **525**:486-490.

30. George JM: **The synucleins**. *Genome Biol* 2002, **3** REVIEWS3002.

31. George JM, Jin H, Woods WS, Clayton DF: **Characterization of a novel protein regulated during the critical period for song learning in the zebra finch**. *Neuron* 1995, **15**:361-372.

32. Perrin RJ, Woods WS, Clayton DF, George JM: **Interaction of human alpha-Synuclein and Parkinson's disease variants with phospholipids. Structural analysis using site-directed mutagenesis**. *J Biol Chem* 2000, **275**:34393-34398.

33. Kruger R, Kuhn W, Muller T, Woitalla D, Graeber M, Kosel S, Przuntek H, Epplen JT, Schols L, Riess O: **Ala30Pro mutation in the gene encoding alpha-synuclein in Parkinson's disease**. *Nat Genet* 1998, **18**:106-108.

34. Zarranz JJ, Alegre J, Gomez-Esteban JC, Lezcano E, Ros R, Ampuero I, Vidal L, Hoenicka J, Rodriguez O, Atares B *et al.*: **The new mutation, E46K, of alpha-synuclein causes Parkinson and Lewy body dementia**. *Ann Neurol* 2004, **55**:164-173.

35. Appel-Cresswell S, Vilarino-Guell C, Encarnacion M, Sherman H, Yu I, Shah B, Weir D, Thompson C, Szu-Tu C, Trinh J *et al.*: **Alpha-synuclein p.H50Q, a novel pathogenic mutation for Parkinson's disease**. *Mov Disord* 2013, **28**:811-813.

36. Lesage S, Anheim M, Letournel F, Bousset L, Honore A, Rozas N, Pieri L, Madiona K, Durr A, Melki R *et al.*: **G51D alpha-synuclein mutation causes a novel parkinsonian-pyramidal syndrome**. *Ann Neurol* 2013, **73**:459-471.

37. Pasanen P, Myllykangas L, Siitonen M, Raunio A, Kaakkola S, Lyytinen J, Tienari PJ, Poyhonen M, Paetau A: **Novel alpha-synuclein mutation A53E associated with atypical multiple system atrophy and Parkinson's disease-type pathology**. *Neurobiol Aging* 2014, **35**:2180.e1-2180.e5.

38. Yoshino H, Hirano M, Stoessl AJ, Imamichi Y, Ikeda A, Li Y, Funayama M, Yamada I, Nakamura Y, Sossi V *et al.*: **Homozygous alpha-synuclein p.A53V in familial Parkinson's disease**. *Neurobiol Aging* 2017, **57**:248.e7-248.e12.

39. Polymeropoulos MH, Lavedan C, Leroy E, Ide SE, Dehejia A, Dutra A, Pike B, Root H, Rubenstein J, Boyer R *et al.*: **Mutation in the alpha-synuclein gene identified in families with Parkinson's disease**. *Science* 1997, **276**:2045-2047.

40. Giasson BI, Murray IV, Trojanowski JQ, Lee VM: **A hydrophobic stretch of 12 amino acid residues in the middle of alpha-synuclein is essential for filament assembly**. *J Biol Chem* 2001, **276**:2380-2386.

41. Ueda K, Fukushima H, Masliah E, Xia Y, Iwai A, Yoshimoto M, Otero DA, Kondo J, Ihara Y, Saitoh T: **Molecular cloning of cDNA encoding an unrecognized component of amyloid in Alzheimer disease**. *Proc Natl Acad Sci U S A* 1993, **90**:11282-11286.

42. Li HT, Du HN, Tang L, Hu J, Hu HY: **Structural transformation and aggregation of human alpha-synuclein in trifluoroethanol: non-amyloid component sequence is essential and beta-sheet formation is prerequisite to aggregation**. *Biopolymers* 2002, **64**:221-226.

43. Li WW, Yang R, Guo JC, Ren HM, Zha XL, Cheng JS, Cai DF: **Localization of alpha-synuclein to mitochondria within midbrain of mice**. *Neuroreport* 2007, **18**:1543-1546.

44. Post MR, Lieberman OJ, Mosharov EV: **Can interactions between α-synuclein, dopamine and calcium explain selective neurodegeneration in Parkinson's disease?** *Front Neurosci* 2018, **12**:161.

45. Li W, West N, Colla E, Pletnikova O, Troncoso JC, Marsh L, Dawson TM, Jakala P, Hartmann T, Price DL *et al.*: **Aggregation promoting C-terminal truncation of alpha-synuclein is a normal cellular process and is enhanced by the familial Parkinson's disease-linked mutations**. *Proc Natl Acad Sci U S A* 2005, **102**:2162-2167.

46. Liu CW, Giasson BI, Lewis KA, Lee VM, Demartino GN, Thomas PJ: **A precipitating role for truncated alpha-synuclein and the proteasome in alpha-synuclein aggregation: implications for pathogenesis of Parkinson disease**. *J Biol Chem* 2005, **280**:22670-22678.

47. Crowther RA, Jakes R, Spillantini MG, Goedert M: **Synthetic filaments assembled from C-terminally truncated alpha-synuclein**. *FEBS Lett* 1998, **436**:309-312.

48. Wang W, Nguyen LTT, Burlak C, Chegini F, Guo F, Chataway T, Ju S, Fisher OS, Miller DW, Datta D *et al.*: **Caspase-1 causes truncation and aggregation of the Parkinson's disease-associated protein α-synuclein**. *Proc Natl Acad Sci U S A* 2016, **113**:9587-9592.

49. Chen M, Margittai M, Chen J, Langen R: **Investigation of alpha-synuclein fibril structure by site-directed spin labeling**. *J Biol Chem* 2007, **282**:24970-24979.

50. Miake H, Mizusawa H, Iwatsubo T, Hasegawa M: **Biochemical characterization of the core structure of alpha-synuclein filaments**. *J Biol Chem* 2002, **277**:19213-19219.

51. •• Guerrero-Ferreira R, Taylor NM, Mona D, Ringler P, Lauer ME, Riek R, Britschgi M, Stahlberg H: **Cryo-EM structure of alpha-synuclein fibrils**. *eLife* 2018, **7**

First structure of aSyn fibrils solved at high resolution by cryo-EM. This study used C-terminally truncated, recombinant fibrils to determine the arrangement of two protofilaments and the location of the familial PD mutation sites. It also proposes a hypothesis for how the hydrophobic regions within each protofilament may drive aSyn aggregation and fibril growth.

52. •• Li Y, Zhao C, Luo F, Liu Z, Gui X, Luo Z, Zhang X, Li D, Liu C, Li X: **Amyloid fibril structure of α-synuclein determined by cryo-electron microscopy**. *Cell Res* 2018, **28**:897-903

Structure of full-length aSyn solved by cryo-EM. The map allowed for a larger coverage of residues in the atomic model. This study combined cryo-EM with Atomic Force Microscopy to determine chirality, thickness and periodicity on a variety of fibrils including wild-type and some with familial PD mutations.

53. •• Li B, Ge P, Murray KA, Sheth P, Zhang M, Nair G, Sawaya MR, Shin WS, Boyer DR, Ye S *et al.*: **Cryo-EM of full-length α-synuclein reveals fibril polymorphs with a common structural kernel**. *Nat Commun* 2018, **9**:3609

Two new polymorphs of aSyn were solved to a resolution of 3.7 Å using cryo-EM. Both forms share a kernel structure but their filaments interact in different ways. The rod polymorph's protofilaments interact via the preNAC steric zipper, whereas the twister polymorph's inter-protofilament interface is in the NACore region of aSyn.

54. •• Boyer DR, Li B, Sun C, Fan W, Sawaya MR, Jiang L, Eisenberg DS: **Structures of fibrils formed by α-synuclein hereditary disease mutant H50Q reveal new polymorphs**. *Nat Struct Mol Biol* 2019, **26**:1044-1052

The authors present the cryo-EM structure of fibrils formed by alpha-synuclein carrying the H50Q mutation. They found two polymorphs of aSyn called Narrow (single protofilament) and Wide (two protofilaments) fibrils. Since the solid-state NMR structure published in 2017, this is the first high-resolution structure of aSyn fibrils formed by a single protofilament.

55. •• Guerrero-Ferreira R, Taylor NMI, Arteni A-A, Kumari P, Mona D, Ringler P, Britschgi M, Lauer ME, Verasdock J, Riek R *et al.*: **Two new polymorphic structures of alpha-synuclein solved by cryo-electron microscopy**. *eLife* 2019, **8**:48907

This research reports two aSyn polymorphs (2a and 2b) composed of two protofilaments. Both types are the result of changes in the individual aSyn fold instead of a simple rearrangement of individual protofilaments. This work shows that aSyn can form more than one monomeric organization. In these polymorphs, some of the familial PD mutation sites define the inter-protofilament interface.

56. Oueslati A, Fournier M, Lashuel HA: **Chapter 7 - role of post-translational modifications in modulating the structure, function and toxicity of α-synuclein: implications for Parkinson's disease pathogenesis and therapies**. In *Progress in Brain Research*, , vol 183. Edited by Björklund A, Cenci MA. Elsevier; 2010:115-145.

57. Hasegawa M, Fujiwara H, Nonaka T, Wakabayashi K, Takahashi H, Lee VM, Trojanowski JQ, Mann D, Iwatsubo T: **Phosphorylated alpha-synuclein is ubiquitinated in alpha-synucleinopathy lesions**. *J Biol Chem* 2002, **277**:49071-49076.

58. Nonaka T, Iwatsubo T, Hasegawa M: **Ubiquitination of alpha-synuclein**. *Biochemistry* 2005, **44**:361-368.

59. Iyer A, Roeters SJ, Schilderink N, Hommersom B, Heeren RM, Woutersen S, Claessens MM, Subramaniam V: **The impact of N-terminal acetylation of alpha-synuclein on phospholipid membrane binding and fibril structure**. *J Biol Chem* 2016, **291**:21110-21122.

60. Maltsev AS, Ying J, Bax A: **Impact of N-terminal acetylation of alpha-synuclein on its random coil and lipid binding properties**. *Biochemistry* 2012, **51**:5004-5013.

61. Oueslati A, Paleologou KE, Schneider BL, Aebischer P, Lashuel HA: **Mimicking phosphorylation at serine 87 inhibits the aggregation of human alpha-synuclein and protects against its toxicity in a rat model of Parkinson's disease**. *J Neurosci* 2012, **32**:1536-1544.

62. Paleologou KE, Oueslati A, Shakked G, Rospigliosi CC, Kim HY, Lamberto GR, Fernandez CO, Schmid A, Chegini F, Gai WP *et al.*: **Phosphorylation at S87 is enhanced in synucleinopathies, inhibits alpha-synuclein oligomerization, and influences synuclein-membrane interactions**. *J Neurosci* 2010, **30**:3184-3198.

63. De Rosier DJ, Klug A: **Reconstruction of three dimensional structures from electron micrographs**. *Nature* 1968, **217**:130-134.

64. Owen CH, Morgan DG, DeRosier DJ: **Image analysis of helical objects: the Brandeis Helical Package**. *J Struct Biol* 1996, **116**:167-175.

65. Egelman EH: **The iterative helical real space reconstruction method: surmounting the problems posed by real polymers**. *J Struct Biol* 2007, **157**:83-94.

66. Whittaker M, Carragher BO, Milligan RA: **PHOELIX: a package for semi-automated helical reconstruction**. *Ultramicroscopy* 1995, **58**:245-259.

67. Desfosses A, Ciuffa R, Gutsche I, Sachse C: **SPRING - an image processing package for single-particle based helical reconstruction from electron cryomicrographs**. *J Struct Biol* 2014, **185**:15-26.

68. Scheres SH: **RELION: implementation of a Bayesian approach to cryo-EM structure determination**. *J Struct Biol* 2012, **180**:519-530.

69. • He S, Scheres SHW: **Helical reconstruction in RELION**. *J Struct Biol* 2017, **198**:163-176

A comprehensive manuscript describing the implementation of a helical reconstruction method within the RELION software. In this manuscript, four sample datasets are used to test a number of parameters and reconstruction procedures. This work explains in detail the functionality of the helical reconstruction implementation and gives examples for how to improve resolution, calculate appropriate initial parameters for particle extraction, 2D and 3D classification and 3D refinement, in addition to instructions on how to determine an adequate initial model.

70. Bepler T, Morin A, Noble AJ, Brasch J, Shapiro L, Berger B: **Positive-unlabeled convolutional neural networks for particle picking in cryo-electron micrographs**. *Res Comput Mol Biol* 2018, **10812**:245-247.

71. Wagner T, Merino F, Stabrin M, Moriya T, Antoni C, Apelbaum A, Hagel P, Sitsel O, Raisch T, Prumbaum D *et al.*: **SPHIRE-crYOLO is a fast and accurate fully automated particle picker for cryo-EM**. *Commun Biol* 2019, **2**:218.

72. Scheres SHW: **Amyloid structure determination in RELION-3.1**. *Act Cryst D Struct Biol* 2020, **76**:94-101.